Organometallics **2006,** *25,* 4366−4373

Structural Diversity of Organoantimony(III) and Organobismuth(III) Dihalides Containing O,C,O-Chelating Ligands

Libor Dostál,*,[†] Ivana Císařová,[‡] Roman Jambor,[†] Aleš Růžička,[†] Robert Jirásko,[§] and
Jaroslav Holeček[†]

Department of General and Inorganic Chemistry and Department of Analytical Chemistry, Faculty of Chemical Technology, University of Pardubice, nám. Čs. legií 565, CZ - 532 10, Pardubice, Czech Republic, and Faculty of Natural Science, Charles University in Prague Hlavova 2030, CZ-128 40, Prague 2, Czech Republic

Received June 5, 2006

Eight organoantimony and organobismuth dihalides, containing two types of O,C,O-chelating (so-called pincer) ligands, 2,6-$(ROCH_2)C_6H_3^-$ (R = Me, L^1; R = ^{t}Bu, L^2; L^1SbCl_2 (**1**), L^2SbCl_2 (**2**), L^1SbI_2 (**3**), L^2SbI_2 (**4**), L^1BiCl_2 (**5**), L^2BiCl_2 (**6**), L^1BiI_2 (**7**), L^2BiI_2 (**8**)) were prepared and characterized with the help of elemental analysis, electrospray ionization mass spectrometry, ^{1}H and ^{13}C NMR spectroscopy, and X-ray diffraction techniques. Except for **5**, which exists as a centrosymmetric dimer, all studied compounds are monomeric in the solid state and the coordination polyhedra of the central atoms are distorted square-pyramidal. Both oxygen donor atoms are coordinated to the central metal through moderately strong or strong intramolecular interactions (range of Sb−O distances 2.279(2)−2.6912(14) Å and Bi−O distances 2.379(3)−2.460(4) Å), both in *cis* fashion for **1** and **2** (angles O−Sb−O 116.65(5)° and 116.73(4)°) and *trans* fashion for **3**, **4**, and **6**−**8** (range of angles O−M−O; M = Sb or Bi, 142.26(12)−148.28(8)°). In noncoordinating solvents ($CDCl_3$, toluene-d_8) **1**−**8** display structures similar to those found in the solid state based on variable-temperature ^{1}H NMR measurements.

Introduction

The chemistry of hypervalent compounds has received much attention in organometallic chemistry, and rapid development of this area has taken place in recent years.[1] The use of aromatic ligands bearing one or two *ortho*-pendant functional group(s) with potential ability for intramolecular coordination, so-called C,Y or Y,C,Y (Y = appropriate donor atom) chelating ligands, is a common approach for stabilization of both transition[2] and main group metal complexes.[3] Many such complexes containing these ligands displayed unusual geometries at the central metal atom and/or solid-state structures.

Recently the chemistry of hypervalent compounds bearing heavier pnictogens (in particular Sb, Bi) has attracted interest as well. The majority of these complexes contain C,N ligands. For example, 2-$(Me_2NCH_2)C_6H_4^-$ and 8-$(Me_2N)C_{10}H_6^-$ moieties have often been applied to stabilize organoantimony and organobismuth molecular complexes,[4] cations,[5] or compounds containing metal−metal bonds.[4f,i,6] The utilization of 2,6-$(Me_2NCH_2)_2C_6H_3^-$ as an N,C,N-type representative for this purpose was somewhat less frequent.[7]

In contrast to the common occurrence of Sb−N or Bi−N intramolecular interactions only few examples of complexes with

---

* To whom correspondence should be addressed. E-mail: libor.dostal@upce.cz.

[†] Department of General and Inorganic Chemistry, University of Pardubice.

[‡] Charles University in Prague.

[§] Department of Analytical Chemistry, University of Pardubice.

(1) *Chemistry of Hypervalent Compounds*; Akiba, K.-Y., Ed.; Wiley-VCH: New York, 1999.

(2) For example see: (a) Albrecht, M.; van Koten, G. *Angew. Chem., Int. Ed.* **2001**, *40*, 3750. (b) van der Boom, M. E.; Milstein, D. *Chem. Rev.* **2003**, *103,* 1759. (c) van Koten, G. *Pure Appl. Chem.* **1989**, *61,* 1681. (d) Frech, C. M.; Shimon, L. J. W.; Milstein, D. *Angew. Chem., Int. Ed.* **2005**, *44,* 1709. (e) Gandelman, M.; Shimon, L. J. W.; Milstein, D. *Chem. Eur. J.* **2003**, *9*, 4295. (f) Poverenov, E.; Gandelman, M.; Shimon, L. J. W.; Rozenberg, H.; Ben-David, Y.; Milstein, D. *Chem. Eur. J.* **2004**, *10*, 4673. (g) Kossoy, E.; Iron, M. A.; Rybtchinski, B.; Ben-David, Y.; Shimon, L. J. W.; Konstantinovski, L.; Martin J. M. L.; Milstein, D. *Chem. Eur. J.* **2005**, *11*, 2319. (h) Slagt, M. Q.; van Zwieten, D. A. P.; Moerkerk, A. J. C. M.; Gebbing, R. J. M. K.; van Koten, G. *Coord. Chem. Rev.* **2004**, *248*, 2275.

(3) For example see: (a) Gossage, R. A.; Jastrzebski, J. T. B. H.; van Koten, G. *Angew. Chem., Int. Ed.* **2005**, *44*, 1448. (b) Kronenburg, C. P. M.; Rijnberg, E.; Jastrzebski, J. T. B. H.; Kooijman, H.; Lutz, M.; Spek, A. L.; Gossage, R. A.; van Koten, G. *Chem. Eur. J.* **2004**, *10*, 253. (c) Jastrzebski, J. T. B. H.; van Koten, G. *Adv. Organomet. Chem.* **1993**, *35*, 241. (d) Arink, A. M.; Kronenburg, C. P. M.; Jastrzebski, J. T. B. H.; Lutz, M.; Spek, A. L.; Gossage, R. A.; van Koten, G. *J. Am. Chem. Soc.* **2004**, *126*, 16249. (e) Chauhan, M.; Chuit, C.; Corriu, R. J. P.; Mehdi, A.; Reye, C. *Organometallics* **1996**, *15*, 4326. (f) Carre, F.; Chuit, C.; Corriu, R. J. P.; Fanta, A.; Mehdi, A.; Reye, C. *Organometallics* **1995**, *14*, 194. (g) Peveling, K.; Henn, M.; Löw, C.; Mehring, M.; Schürmann, M.; Costisella, B.; Jurkschat, K. *Organometallics* **2004**, *23*, 1501. (h) Mehring, M.; Vrasidas, I.; Horn, D.; Schürmann, M.; Jurkschat, K. *Organometallics* **2001**, *20*, 4647. (i) Růžička, A.; Jambor, R.; Císařová, I.; Holeček, J. *Chem. Eur. J.* **2003**, *9*, 2411. (j) Dostál, L.; Jambor, R.; Růžička, A.; Jirásko, R.; Císařová, I.; Holeček, J. *J. Organomet. Chem.* **2006**, *691*, 35.

(4) (a) Kamepalli, S.; Carmalt, C. J.; Culp, R. D.; Cowley, A. H.; Jones, R. A. *Inorg. Chem.* **1996**, *35*, 6179. (b) Suzuki, H.; Murafuji, T.; Matano, Y.; Azuma, N. *J. Chem. Soc., Perkin Trans. 1* **1993**, 2969. (c) Murafuji, T.; Azuma, N.; Suzuki, H. *Organometallics* **1995**, *14*, 1542. (d) Carmalt, C. J.; Cowley, A. H.; Culp, R. D.; Jones, R. A.; Kamepalli, S.; Norman, C. N. *Inorg. Chem.* **1997**, *36*, 2770. (e) Sharma, P.; Castillo, D.; Rosas, N.; Cabrera, A.; Gomez, E.; Toscano, A.; Lara, F.; Hernández, S.; Espinosa, G. *J. Organomet. Chem.* **2004**, *689*, 2593. (f) Opris, L. M.; Silvestru, A.; Silvestru, C.; Breunig, H. J.; Lork, E. *Dalton Trans.* **2004**, 3575. (g) Balazs, L.; Stanga, O.; Breunig, H. J.; Silvestru, C. *Dalton Trans.* **2003**, 2237. (h) Opris, L. M.; Silvestru, A.; Silvestru, C.; Breunig, H. J.; Lork, E. *Dalton Trans.* **2003**, 4367. (i) Breunig, H. J.; Ghesner, I.; Ghesner, M. E.; Lork, E. *Inorg. Chem.* **2003**, *42*, 1751.

(5) Carmalt, C. J.; Walsh, D.; Cowley, A. H.; Norman, C. N. *Organometallics* **1997**, *16*, 3597.

(6) Balazs, L.; Breunig, H. J.; Lork, E.; Silvestru, C. *Eur. J. Inorg. Chem.* **2003**, 1361.

(7) (a) Atwood, D. A.; Cowley, A. H.; Ruiz, J. *Inorg. Chim. Acta* **1992**, *198*−*200*, 271. (b) Yamamoto, Y.; Chen, X.; Kojima, S.; Ohdoi, K.; Kitano, M.; Doi, Y.; Akiba, K.-Y. *J. Am. Chem. Soc.* **1995**, *117*, 3922. (c) Breunig, H. J. *Z. Anorg. Allg. Chem.* **2005**, *631*, 621. (d) Balazs, L.; Breunig, H. J.; Lork, E.; Soran, A.; Silvestru, C. *Inorg. Chem.* **2006**, *45*, 2341.

10.1021/om060489q CCC: \$33.50

Chart 1

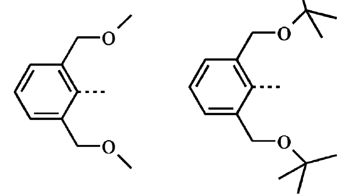

L^1 L^2

Scheme 1. Synthesis of Studied Compounds

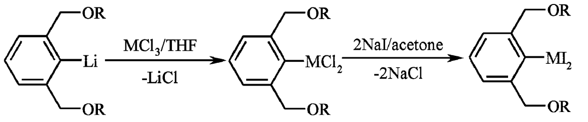

R=Me; M=Sb (**1**)
R=^{t}Bu; M=Sb (**2**)
R=Me; M=Bi (**5**)
R=^{t}Bu; M=Bi (**6**)

R=Me; M=Sb (**3**)
R=^{t}Bu; M=Sb (**4**)
R=Me; M=Bi (**7**)
R=^{t}Bu; M=Bi (**8**)

Sb−O or Bi−O intramolecular coordination have been reported. The presence of an Sb−O intramolecular interaction was found in compounds containing 2-[EtOC(CF$_3$)$_2$]C$_6$H$_4$$^-$ and [2-(O=CH)C$_6$H$_4$]$^-$ coordinating units.[8] The intramolecular Bi−O contacts were established by X-ray crystallography in compounds bearing 2-(^{t}BuSO$_2$)C$_6$H$_4$$^-$,[9] 2-(O=CMe)C$_6H_4$$^-$,[10] 2-(MeO)-C$_6H_4$$^-$,[11] 2,6-(MeO)$_2C_6H_3$$^-$,[12] 2-(MeOCMe$_2$)C$_6H_4$$^-$, and [2-MeOC(CF$_3$)$_2$]C$_6H_4$$^-$ [13] as ancillary ligands.

To develop further the chemistry of compounds containing Sb−O or Bi−O intramolecular interactions, here we report on the synthesis and solution and solid-state structural studies of organoantimony and organobismuth chlorides and iodides containing two types of O,C,O-chelating (so-called pincer) ligands L^1 and L^2 [2,6-(ROCH$_2$)C$_6$H$_3$$^-$; R = Me, L^1; R = ^{t}Bu, L^2;[14] L^{1}SbCl$_2$ (**1**), L^{2}SbCl$_2$ (**2**), L^{1}SbI$_2$ (**3**), L^{2}SbI$_2$ (**4**), L^{1}BiCl$_2$ (**5**), L^{2}BiCl$_2$ (**6**), L^{1}BiI$_2$ (**7**), L^{2}BiI$_2$ (**8**) (Chart 1 and Scheme 1)].

All compounds were characterized by the help of elemental analysis, ^{1}H and ^{13}C NMR spectroscopy, and single-crystal X-ray diffraction. This set of compounds provides the opportunity to study the influence of the central metal, the ligand, and the halide used on the coordination polyhedra in **1**−**8**. The strength of the coordination of the donor groups CH$_2$OR to the metal (antimony or bismuth) center and mutual position of the donor atoms in **1**−**8** were studied as well.

Results and Discussion

Synthetic Aspects. Compounds **1**, **2**, **5**, and **6** were prepared by the reaction of SbCl$_3$ or BiCl$_3$ with the appropriate organolithium derivatives L^{1}Li[14a] and L^{2}Li[15] in THF in moderate yields (Scheme 1). The reaction of the chlorides **1**, **2**, **5**, and **6** thus prepared with 2 equiv of NaI in acetone afforded the corresponding iodides **3**, **4**, **7**, and **8** (Scheme 1). All compounds had satisfactory elemental analysis, and their identities were established by ESI mass spectrometry.

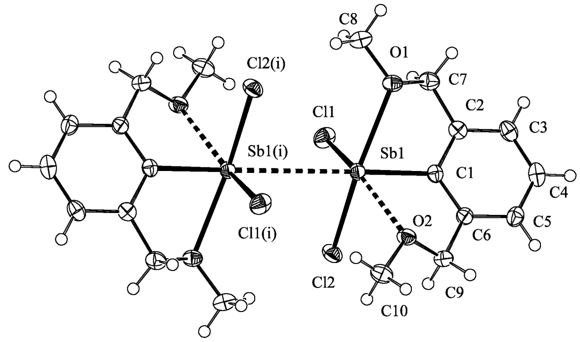

Figure 1. ORTEP plot of molecules of **1** showing 50% probability displacement ellipsoids and the atom-numbering scheme (symmetry code (i): 1−*x*, −*y*, 1−*z*).

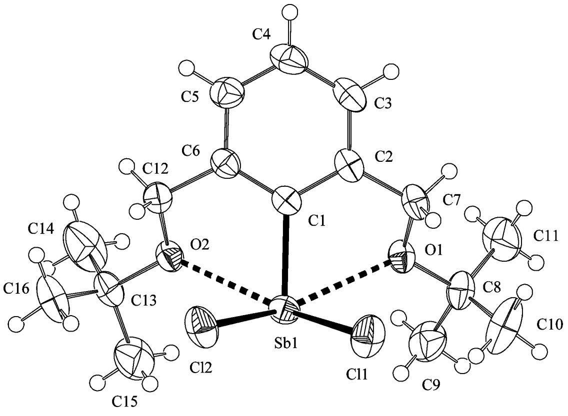

Figure 2. ORTEP plot of a molecule of **2** showing 50% probability displacement ellipsoids and the atom-numbering scheme.

Molecular Structures of 1−8. The molecular structures of **1**−**8** were determined by single-crystal X-ray diffraction and are depicted in Figures 1−8. Selected bond lengths and bonding angles are given in Table 1. For compound **5** the structural parameters are given in the figure caption of Figure 5.

The primary coordination sphere of antimony in **1** is formed by the *ipso* carbon atom of the ligand L^1, two chlorine atoms, and two moderately strongly coordinated oxygen donor atoms, with bond lengths Sb(1)−O(1) 2.577(2) Å and Sb(1)−O(2) 2.523(2) Å shorter than the sum of the van der Waals radii, $\sum_{\mathrm{vdW}}$(Sb,O) = 3.78 Å.[16] These values still indicate stronger Sb−O interaction than had been found in 2-[EtOC(CF$_3$)$_2$]C$_6$H$_4$-Sb(2-OC(CF$_3$)$_2$C$_6$H$_4$).[8a] The overall geometry can be described as distorted square-pyramidal,[17a] where the *ipso*-carbon of L^1 is located in an apical position and Sb(1), O(1), O(2), Cl(1), and Cl(2) form the distorted basal plane (the sum of angles describing the SbO$_2$Cl$_2$ girdle is 353.3°). Oxygen atoms as well as chlorine atoms are coordinated mutually in *cis* positions with angles O(1)−Sb(1)−O(2) of 116.68(6)° and Cl(1)−Sb(1)−Cl(2) of 84.54(2)°. This *cis* position of oxygen atoms is in direct contrast to the structure detected for [2,6-(Me$_2$NCH$_2$)$_2$C$_6$H$_3$]-

---

[8] (a) Wakisaka, Y.; Yamamoto, Y.; Akiba, K.-Y. *Heteroat. Chem.* **2001**, *12*, 33. (b) Sharma, P.; Pérez, D.; Rosas, N.; Cabrera, A.; Toscano, A. *J. Organomet. Chem.* **2006**, *691*, 579.

[9] Suzuki, H.; Murafuji, T.; Azuma, N. *J. Chem. Soc., Perkin Trans. 1* **1993**, 1169.

[10] Murafuji, T.; Mutoh, T.; Satoh, K.; Tsunenari, K.; Azuma, N.; Suzuki, H. *Organometallics* **1995**, *14*, 3848.

[11] Suzuki, H.; Ikegami, T.; Azuma, N. *J. Chem. Soc., Perkin Trans. 1* **1997**, 1609.

[12] Ogawa, T.; Ikegami, T.; Hikasa, T.; Ono, N.; Suzuki, H. *J. Chem. Soc., Perkin Trans. 1* **1994**, 3479.

[13] (a) Yamamoto, Y.; Chen, X.; Akiba, K.-Y. *J. Am. Chem. Soc.* **1992**, *114*, 7906. (b) Chen, X.; Yamamoto, Y.; Akiba, K.-Y. *Heteroat. Chem.* **1995**, *4*, 293. (c) Yamamoto, Y.; Ohdoi, K.; Chen, X.; Kitano, M.; Akiba, K.-Y. *Organometallics* **1993**, *12*, 3297.

[14] (a) Jambor, R.; Dostál, L.; Růžička, A.; Císařová, I.; Brus, J.; Holeček, J. *Organometallics* **2002**, *22*, 3996. (b) Kašná, B.; Jambor, R.; Dostál, L.; Růžička, A.; Císařová, I.; Holeček, J. *Organometallics* **2004**, 23, 5300.

[15] Jambor, R.; Dostál, L.; Růžička, A.; Císařová, I.; Holeček, J. *Inorg. Chim. Acta* **2005**, *358*, 2422.

[16] Spek, A. L. *PLATON*, A Multipurpose Crystallographic Tool; Utrecht University: Utrecht, The Netherlands, 2005; available at http://www.cryst.chem.uu.nl/platon/.

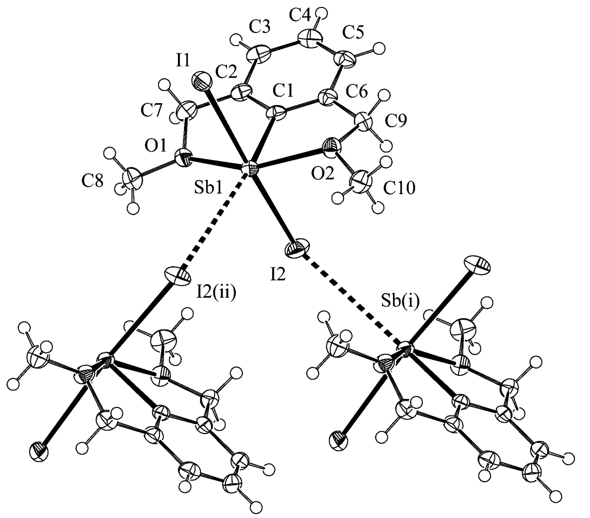

Figure 3. ORTEP plot of molecules of **3** showing 50% probability displacement ellipsoids and the atom-numbering scheme (symmetry code (i): 2−*x*, 1/2+*y*, 1/2−*z*; (ii): 2−*x*, −1/2+*y*, 1/2−*z*).

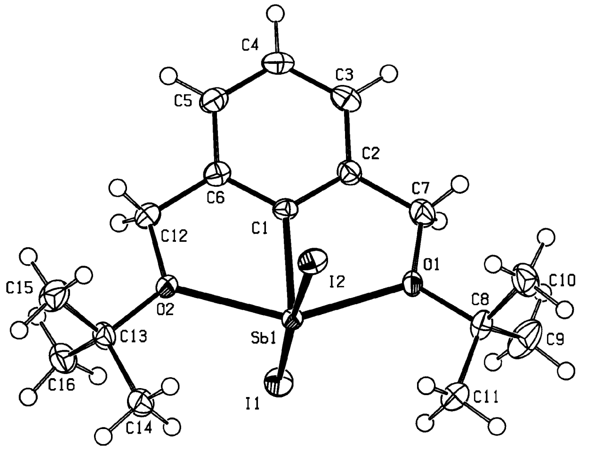

Figure 4. ORTEP plot of molecules of **4** showing 50% probability displacement ellipsoids and the atom-numbering scheme.

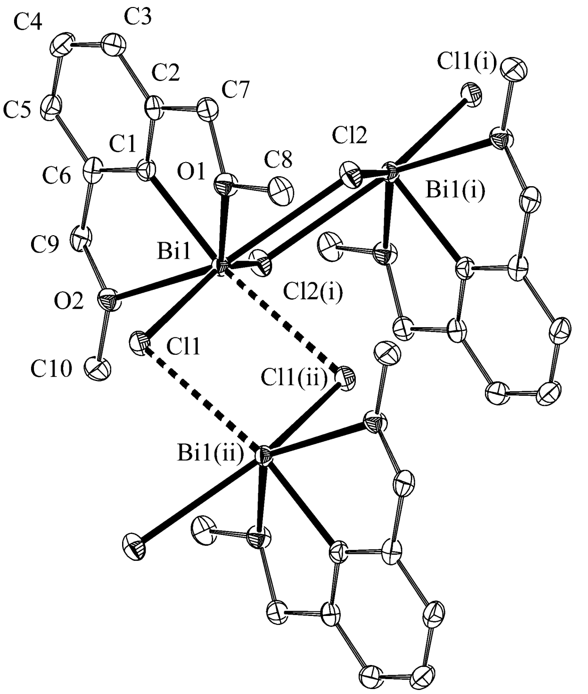

Figure 5. ORTEP plot of molecules of **5** showing 50% probability displacement ellipsoids and the atom-numbering scheme (symmetry code (i): 1−*x*, 1−*y*, 1−*z*; (ii): 2−*x*, 1−*y*, 1−*z*). Hydrogen atoms were omitted for clarity. Selected bond lengths (Å) and angles (deg): Bi(1)−C(1) 2.222(4), Bi(1)−Cl(1) 2.6595(1), Bi(1)−Cl(2) 2.8873(1), Bi(1)−Cl(2i) 2.8850(1), Bi(1)−O(1) 2.493(3), Bi(1)−O(2) 2.501(3), Bi(1)−Cl(2)−Bi(1i) 105.46(3), Cl(2)−Bi(1)−Cl(2i) 74.54(3), Cl(1)−Bi(1)−Cl(2) 142.28(3), Cl(1)−Bi(1)−Cl(2i) 140.26(3), O(1)−Bi(1)−O(2) 127.50(10), O(1)−Bi1−C(1) 69.24(12), O(2)−Bi(1)−C(1) 69.17(12).

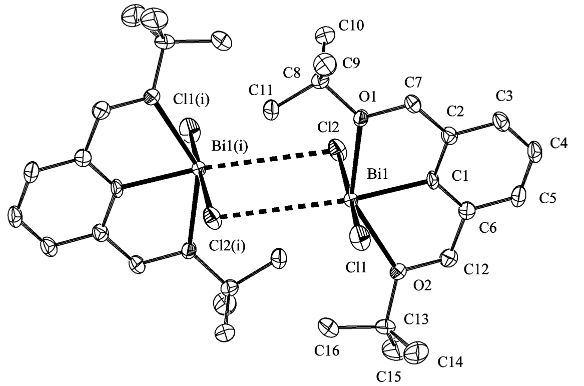

Figure 6. ORTEP plot of molecules of **6** showing 50% probability displacement ellipsoids and the atom-numbering scheme (symmetry code (i): 2−*x*, −*y*, 1−*z*). Hydrogen atoms were omitted for clarity.

$SbCl_2$, where both nitrogen donor atoms are in the resulting square-pyramid located in *trans* fashion, with an N−Sb−N angle of 147.3(3)°.[7a] An almost analogous structure with weaker Sb−O interactions was observed also for derivative **2** (Figure 2, Table 1). The remarkable feature of the solid-state structure of **1** is an intermolecular contact between two antimony atoms of centrosymmetrically related molecules with an Sb···Sb distance of 3.7371(3) Å, significantly shorter than the sum of the van der Waals radii, $\sum_{vdW}(Sb,Sb) = 4.52$ Å.[16] The Sb···Sb contact is located *trans* to the Sb(1)−C(1) bond and formally completes a distorted octahedron around Sb(1). Such a short intermolecular distance between antimony atoms is not rare. More then 200 crystal structures with Sb···Sb distances within the interval 3.0−4.2 Å were found in CSD.[18] However, in most cases the molecules have been brought into each other's vicinity also by the interaction between antimony and the other atom of the adjacent molecule.[4d,19]

Therefore, the additional geometric restrictions were added to the search of the database to ensure the Sb···Sb interaction

---

(17) (a) This structure can also be described as a *ψ*-octahedron, if the lone pair of the central metal is included in the overall geometry. This lone pair is then located in *trans* position to the *ipso*-carbon atom of the ligands $L^{1,2}$. The third possible description of the coordination polyhedron in **1** and **2** is as a trigonal pyramid at the central antimony atom formed by Sb(1), C(1), Cl(1), and Cl(2) (the sum of angles describing the $SbCCl_2$ girdle is 279.7° for **1** and 277.9° for **2**) bicapped by two oxygen donor atoms. (b) This structure also can be described as a *ψ*-octahedron, if the lone pair of the central metal is included in the overall geometry. This lone pair is then located in *trans* position to the *ipso*-carbon of the ligands $L^{1,2}$.

(18) Allen, F. H. *Acta Crystallogr.* **2002**, B58, 380.

(19) For examples of compounds containing Sb···Sb contacts see: (a) Avarvari, N.; Faulques, E.; Fourmingué, M. *Inorg. Chem.* **2001**, *40*, 2570. (b) Hill, A. M.; Levason, W.; Webster, M.; Albert, I. *Organometallics* **1997**, *16*, 6, 5641. (c) Silvestru, C.; Haiduc, I.; Kaller, R.; Ebert, K. H.; Breunig, H. J. *Polyhedron* **1993**, *12*, 2611. (d) Breunig, H. J.; Burford, N.; Rösler, R. *Angew. Chem. Int. Ed.* **2000**, *39*, 4148. (e) Hughbanks, T.; Hoffmann, R.; Whangbo, M. H.; Stewart, K. R.; Eisenstein, O.; Canadell, E. *J. Am. Chem. Soc.* **1982**, *104*, 3876. (f) Grobe, J.; Golla, W.; Van, D. L.; Krebs, B.; Läge, M. *Organometallics* **1998**, *17*, 7, 5717. (g) Breunig, H. J.; Rösler, R.; Lork, E. *Angew. Chem., Int. Ed. Engl.* **1997**, *36*, 2819. (h) Stahler, R.; Bensch, W.; *Eur. J. Inorg. Chem.* **2001**, 3073. (i) Davies, J. E.; Mays, M. J.; Raithby, P. R.; Shields, G. P.; Tompkin, P. K.; Woods, A. D. *J. Chem. Soc., Dalton Trans.* **2000**, 1925.

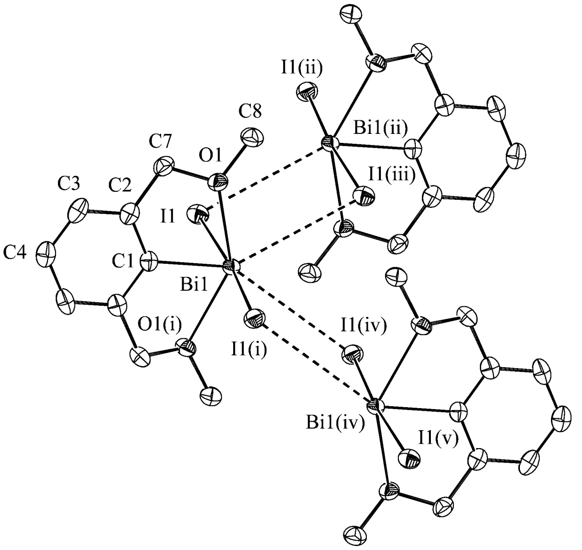

Figure 7. ORTEP plot of molecules of **7** showing 50% probability displacement ellipsoids and the atom-numbering scheme (symmetry code (i): $-x, y, -z+1/2$; (ii): $-x, 1-y, 1-z$; (iii): $x, 1-y, -1/2+z$). Hydrogen atoms were omitted for clarity.

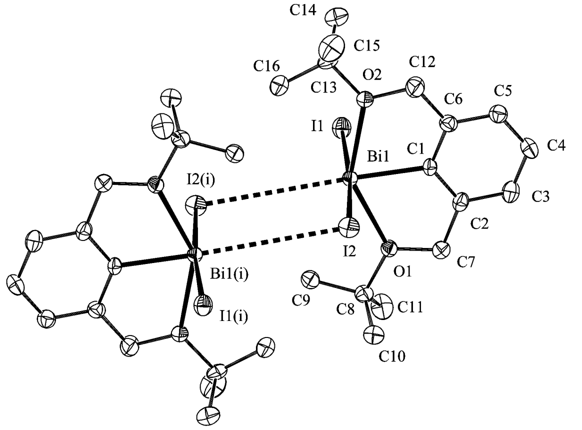

Figure 8. ORTEP plot of molecules of **8** showing 50% probability displacement ellipsoids and the atom-numbering scheme (symmetry code (i): $1-x, -y, 2-z$). Hydrogen atoms were omitted for clarity.

conforms to such restrictions (angles L-Sb···Sb′ and Sb···Sb′−L′ within the interval 170−180°). Both conditions are met only by the eight crystal structures, and it is a point of interest that most of them are distibines,[20] where the Sb···Sb intermolecular interactions are very strong; these therefore have been extensively studied. The reason the molecules of **1** are staggered in the same way is probably due to the lack of any other intermolecular interaction, which enables significantly weaker Sb···Sb contacts such as undistorted ones to be identified. This idea is further supported by the crystal packing of **2**, where the Sb···Sb interaction is prevented by the space-demanding *tert*-butyl moiety and no other contact is taking place. Consequently, the unanchored molecules acquire large displacement parameters (Figure 2).

A completely reversed arrangement of oxygen donor atoms and halogens was observed in the crystal structure of **3** (Figure 3). While the resulting polyhedron in **3** is again a distorted square-pyramid[17b] similar to **1** and **2** (with the *ipso*-carbon atom of L^1 in the apical position with an almost ideal basal plane SbO_2I_2; the sum of angles describing the SbO_2I_2 girdle is 357°), both oxygen and iodine atoms are coordinated in *trans* fashion with angles O(1)−Sb(1)−O(2) of 148.28(8)° and I(1)−Sb(1)−I(2) of 174.047(9)°. The bond distances Sb(1)−O(1) = 2.293(2) Å and Sb(1)−O(2) = 2.279(2) Å for **3** approximate the sum of the respective covalent radii, $\sum_{cov}(Sb,O) = 2.14$ Å, and are considerably shorter than $\sum_{vdW}(Sb,O) = 3.78$ Å,[16] indicating strong Sb−O intramolecular interactions in **3**. The structure of the more sterically demanding analogue **4** closely resembles that of **3**, and only weaker Sb−O interactions were established (Figure 4, Table 1).

Both possible structural isomers, *cis* and *trans*, of $[ArMX_2L_2]$ (M = Sb, Bi) are often assumed to have similar stabilities.[21] Although the preference of oxygen donor ligands adopting the *cis* form was suggested, there is a lack of general trends, and an obvious explanation for *cis* coordination of both donor atoms in **1** and **2** and *trans* type in **3** and **4** is lacking. Compounds **1**−**4** thus represent organoantimony derivatives that are able to change their coordination mode depending on the halogen used.

There is weak Sb···I intermolecular contact in **3** with a bond length of 3.852 Å ($\sum_{vdW}(Sb,I) = 4.24$ Å,[16] symmetry code: (ii) $2-x, -1/2+y, 1/2-z$), resulting in an infinite chain structure (Figure 3). The Sb···I intermolecular distances found in **3** are comparable to those in $PhSbI_2$ (3.819(1) and 4.078(1) Å),[22] but weaker than those detected in $[2-(Me_2NCH_2)C_6H_4]SbI_2$ (3.505(2) Å).[4h]

The crystal structures of organobismuth chlorides **5** and **6** are depicted in Figures 5 and 6. Both structures differ significantly. Whereas **6** preserves a monomeric structure in the first coordination sphere in the solid state, **5** is built up of centrosymmetric dimers, due to the presence of two nearly symmetrical chlorine bridges formed by Cl(2) and Cl(2i). The resulting planar Bi_2Cl_2 core is characterized by angles Cl(2)−Bi(1)−Cl(2i) = 74.54(3)° and Bi(1)−Cl(2)−Bi(1i) = 105.46(3)°. The terminal chlorine atoms Cl(1) and Cl(1i) are slightly bent away from this plane (torsion angle Bi(1i)−Cl(2)−Bi(1)−Cl(1) = 161.19(4)°, symmetry code (i): $1-x, 1-y, 1-z$). The bonding lengths of Bi(1)−Cl(2) and Bi(1)−Cl(2i), 2.887(1) and 2.885(1) Å, are slightly elongated in comparison to the terminal ones (Bi(1)−Cl(1), Bi(1i)−Cl(1i) = 2.659(1) Å). The resulting shape of the coordination polyhedron of the central metal can be described as distorted bicapped ψ-trigonal-bipyramid. The equatorial plane is formed by Cl(2), Cl(2i), and Cl(1) atoms (the sum of angles describing the $BiCl_3$ girdle = 357.1°); *ipso*-carbon C(1) and the lone pair are then assumed to be located in axial positions. This trigonal-bipyramid is attached by two oxygen donor atoms O(1) and O(2) with bond distances O(1)−Bi(1) = 2.493(3) Å and O(2)−Bi(1) = 2.501(3) Å, indicating stronger dative interactions in **5** ($\sum_{vdW}(Bi,O)$ 3.86 Å)[16] than those found in $PhBiBr_2$(thf) (2.671(8) Å) and $PhBiI_2$(thf) (2.808(17) Å),[23] resulting in coordination number seven for the central metal. Mutual *cis* positions of the donor atoms is demonstrated by the angle O(1)−Bi(1)−O(2) of 127.50(10)°. The coordination number seven for the central atom is further expanded to eight by a symmetric intermolecular interaction involving another chlorine atom, Cl(1ii), and the Bi center (Bi(1)−Cl(1ii) bonding length = 3.445(1) Å, symmetry code (ii): $2-x, 1-y, 1-z$, $\sum_{vdW}$-

---

(20) (a) Ashe, A. J., III; Butler, W.; Diephouse, R. *J. Am. Chem. Soc.* **1981**, *103*, 207. (b) Ashe, A. J., III; Ludwig, E. G.; Oleksyszyn, J. *Organometallics* **1984**, *3*, 337. (c) Roller, S.; Drager, M.; Breunig, H. J.; Ates, M. *J. Organomet. Chem.* **1987**, *329*, 319. (d) Roller, S.; Drager, M.; Breunig, H. J.; Ates, M. *J. Organomet. Chem.* **1989**, *378*, 327.

(21) James, S. C.; Norman, N. C.; Orpen, A. G. *J. Chem. Soc., Dalton Trans.* **1999**, 2837.

(22) Mundt, O.; Becker, G.; Stadelmann, H.; Thurn, H. *Z. Anorg. Allg. Chem.* **1992**, *617*, 59.

(23) Clegg, W.; Errington, R. J.; Fisher, G. A.; Hockless, D. C. R.; Norman, N. C.; Orpen, A. G.; Stratford, S. E. *J. Chem. Soc., Dalton Trans.* **1992**, 1967.

Table 1. Selected Values of Bond Lengths (Å) and Angles (deg) for Compounds 1−4 and 6−8[a]

	1 M = Sb, X = Cl	**2** M = Sb, X = Cl	**3** M = Sb, X = I	**4** M = Sb, X = I	**6** M = Bi, X = Cl	**7** M = Bi, X = I	**8** M = Bi, X = I
M1−C1	2.143(3)	2.1395(19)	2.108(3)	2.111(3)	2.199(4)	2.219(6)	2.206(5)
M1−X1	2.4335(8)	2.4316(7)	2.9945(3)	2.9351(3)	2.6863(11)	3.0326(4)	3.1050(4)
M1−X2	2.4513(7)	2.4212(5)	2.9781(3)	3.0889(3)	2.6872(11)	3.0326(4)^{i}	3.0096(4)
M1−O1	2.523(2)	2.6911(13)	2.293(2)	2.302(2)	2.376(3)	2.460(4)	2.430(4)
M1−O2	2.577(2)	2.6294(14)	2.279(2)	2.343(2)	2.459(3)	2.460(4)^{i}	2.416(3)
O1−M1−O2	116.68(6)	116.73(4)	148.28(8)	148.00(7)	143.55(9)	142.26(12)^{i}	144.02(12)
X1−M1−X2	84.54(2)	84.16(2)	174.047(9)	176.18(1)	172.45(4)	174.820(10)^{i}	175.163(12)
C1−M1−O1	70.14(8)	67.99(6)	74.06(10)	74.30(10)	72.37(13)	71.12(8)	71.79(15)
C1−M1−O2	69.01(8)	69.47(6)	74.24(10)	73.76(10)	71.26(13)	71.12(8)^{i}	72.29(16)
C1−M1−X1	97.08(7)	98.22(5)	87.55(8)	92.28(8)	89.49(11)	87.409(7)	91.94(13)
C1−M1−X2	98.01(5)	95.56(5)	86.95(8)	91.10(8)	91.54(11)	87.409(7)^{i}	92.41(9)

[a] Symmetry code: (i) −*x*, *y*, 0.5−*z*.

(Bi,Cl) = 4.09 Å[16]), leading to formation of an infinite chain (Figure 5). A similar structure containing dimeric units linked together via additional Bi···X intermolecular contacts was observed in $[2\text{-}(Me_2NCH_2)C_6H_4]BiI_2$,[4d] $PhBiBr_2$,[24a] and $[BiI_3(hmpa)]$.[24b]

The resulting geometry around the central bismuth atom in **6** can be defined as a distorted square-pyramid,[17b] with both oxygen and chlorine atoms located in the BiO_2Cl_2 basal plane (the sum of angles describing the BiO_2Cl_2 girdle = 360.61°) mutually in *trans* positions with angles Cl(1)−Bi(1)−Cl(2) and O(1)−Bi(1)−O(2) of 172.45(4)° and 143.55(9)°, respectively. This is in contrast to **5**, where a *cis* position of donor atoms was found. This structural diversity is similar to that found for **1** and **3**, vide supra. Both oxygen atoms are coordinated to the central metal through stronger intramolecular interactions, O(1)−Bi(1) = 2.376(3) Å and O(2)−Bi(1) = 2.459(3) Å, in **6** than in **5**. The molecular packing is affected by a weak intermolecular contact of Cl(2i)···Bi(1) (3.744(1) Å), resulting in dimeric units similar to those found in **5**; however further condensation into a chain structure is prevented by the *tert*-butyl moiety (Figure 6).

Compound **7** (Figure 7) has a structure with two coordinated oxygen donor atoms, O(1)−Bi(1) = 2.460(3) Å, in *trans* orientation as the symmetry of the molecule follows a 2-fold axis, with the angle O(1)−Sb(1)−O(1i) = 142.23(16)°, resulting in a distorted square-pyramid[17b] environment around the central atom (the sum of angles describing the BiO_2I_2 girdle is 356.64°). The structure and related structural parameters of **8** closely resemble those of **7** (Figure 8, Table 1). A remarkable feature of the structure of **8** is the stronger intramolecular coordination of both donor atoms, O(1)−Bi(1) = 2.430(4) Å and O(2)−Bi(1) = 2.416(4) Å, in comparison to **7**, although the more sterically demanding ligand L^2 is incorporated.

Closer inspection of the crystal structure of **7** shows weak intermolecular contacts of both iodine atoms to the bismuth atoms from the adjacent molecules (Bi−I bonding length = 3.973 Å, $\sum_{vdW}$(Bi,I) = 4.32 Å[16]), leading to formation of an infinite chain similar to that found in compound **5** (Figure 7) and coordination number seven for the central metal. This analogy is preserved also in **8**, where two symmetrical intermolecular contacts I(2i)···Bi(1) (4.2779(5) Å, symmetry code (i): 1−*x*, −*y*, 2−*z*) form a dimer similar to **6**.

Solution NMR Study. ^1H NMR spectra of derivatives **1** and **2** showed one set of sharp signals for both CH_2O and CH_3 groups at room temperature in $CDCl_3$ and toluene-d_8 for **1** and toluene-d_8 for **2** that are split into an AX pattern (CH_2O) at low temperature. These findings indicate the well-known fluxional process of dissociation−association of both ligands' arms[25] at higher temperature (Scheme 2A), which is slowed at low-temperature, resulting in *cis* coordination of both donor atoms[14a] and structures similar to those found for **1** and **2** in the solid state, vide supra. The activation energy of these processes was estimated to be $\Delta G^{\ddagger}(CDCl_3) = 44.6$ kJ mol^{-1}, $\Delta G^{\ddagger}$(toluene-d_8) = 38.8 kJ mol^{-1} for **1** and $\Delta G^{\ddagger}$(toluene-d_8) = 37.0 kJ mol^{-1} for **2** using the Eyring equation.[26] One set of very broad signals for both CH_2O and CH_3 groups was detected in the ^1H NMR spectra of **2** in $CDCl_3$ at room temperature. However, no decoalescence was observed by variable-temperature ^1H NMR spectroscopy. Rather the second set of signals emerged at 280 K in addition to that detected at room temperature and became more intense with decreasing temperature. The signal due to the CH_2O groups is shifted to lower field, $\delta(^1H, CH_2O) = 5.18$ ppm, in the new set in comparison to the original one, $\delta(^1H, CH_2O) = 5.02$ ppm, indicating stronger Sb−O intramolecular interaction.[3c,14b,27] This process leads to the complete transformation of the first broadened set of signals at room temperature to the new one at 235 K. This is then invariable even at 215 K, indicating symmetrical (*trans*) coordination of both ligands' arms. The whole process can be most reasonably explained as transformation of *cis* coordination of both donor atoms at ambient temperature to symmetrical *trans* at low temperature (Scheme 2B). Similar reinforcement of intramolecular interaction in solution leading to an ionization of organotin derivatives was detected in compounds containing similar types of chelating ligands.[3i,27] The equilibrium constants $K = [B]/[A]$ ([A] represent the relative concentration of the *cis* isomer and [B], that of the *trans* isomer) were evaluated directly from the ^1H NMR spectra of **2** below 280 K, when both species were

Scheme 2. Dynamic Processes of Compounds 1 and 2 in Solution

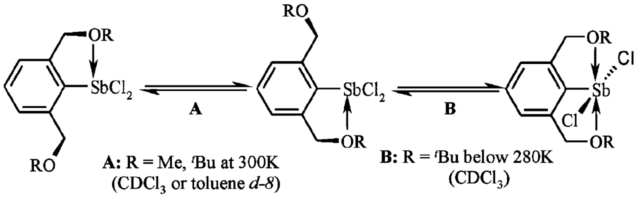

---

[24] (a) Clegg, W.; Errington, R. J.; Fisher, G. A.; Norman, N. C. *J. Mater. Chem.* **1994**, *4*, 891. (b) Clegg, W.; Farrugia, L. J.; McCamley, A.; Norman, N. C.; Orpen, A. G.; Pickett, N. L.; Stratford, S. E. *J. Chem. Soc., Dalton Trans.* **1993**, 2579.

[25] Handwerker, H.; Leis, C.; Probst, R.; Bassinger, P.; Grohmann, A.; Kiprof, P.; Herdtweek, F.; Blümel, J.; Auner, N.; Zybill, C. *Organometallics* **1993**, *12*, 2162.

[26] Eyring equation: $\Delta G^{\ddagger} = -RT_c \ln[2\pi(\Delta\nu)/kT_c\sqrt{3}]$, with $\Delta G^{\ddagger}$ = free energy of activation (J), T_c = coalescence temperature (K), and $\Delta\nu$ = chemical shift difference (Hz); the other symbols have their usual meanings.

[27] Kašná, B.; Jambor, R.; Dostál, L.; Císařová, I.; Holeček, J. *Organometallics* **2006**, *25*, 148.

detected. The K values were evaluated at a number of temperatures and used for a ln K vs T^{-1} plot (see Supporting Information), and the linear relation ($R^2 = 0.9868$) enables us to calculate the reaction enthalpy and entropy: $\Delta H° = -12.9$ kJ mol^{-1}, $\Delta S° = -41.9$ J mol^{-1} K^{-1}.

All variable-temperature ^{1}H NMR spectra of **3**−**8** in $CDCl_3$ solution contain only one set of sharp signals for CH_2O and methyl groups, indicating symmetrical (*trans*) rigid coordination of both donor oxygen atoms in the entire temperature range (300−215 K) studied and thus similar structures for these derivatives, i.e., square-pyramid with *trans*-placed halogen and oxygen atoms.

Experimental Section

General Procedures. All air- and moisture-sensitive manipulations were carried out under an argon atmosphere using standard Schlenk tube techniques. All solvents were dried by standard procedures and distilled prior to use. ^{1}H and ^{13}C NMR spectra were recorded on Bruker AMX360 and Bruker500 Avance spectrometers, respectively, using 5 mm tuneable broad-band probes. Appropriate chemical shifts in the ^{1}H and ^{13}C NMR spectra were calibrated on the residual signals of the solvents ($CDCl_3$: $\delta(^1H) = 7.27$ ppm and $\delta(^{13}C) = 77.23$ ppm; toluene-d_8: $\delta(^1H) = 2.09$ ppm and $\delta(^{13}C) = 20.40$ ppm). Positive-ion and negative-ion electrospray ionization (ESI) mass spectra were measured on an Esquire 3000 ion trap analyzer (Bruker Daltonics, Bremen, Germany) in the range *m*/*z* 50−1000. The samples were dissolved in acetonitrile (except compound **4**, which was dissolved in a 50% mixture of acetonitrile and dichloromethane for a better signal) and analyzed by direct infusion at a flow rate of 5 μL/min. The ion source temperature was 300 °C, the tuning parameter compound stability was 100% for measuring positive ions and 20% for measuring of negative ions (to improve the signal-to-noise ratio), and the flow rate and the pressure of nitrogen were 4 L/min and 10 psi, respectively. The typical ions that confirmed the presence of studied compounds (M) are $[M - X]^+$ (X = Cl, I) in the positive-ion ESI mass spectra and $[M + X]^-$ (X = Cl, I) in the negative-ion ESI mass spectra. In addition the formation of other unusual adducts is observed in the spectra, such as adducts with water and alkali metal ions $[M + Na + H_2O]^+$ and $[M + K + H_2O]^+$ (in case of compound **6**) and a variety of hydrolyzed adducts (in case of compounds **1** and **3**).

The starting chemicals ^{n}BuLi (1.6 M hexane solution), $SbCl_3$ (99.99%), $BiCl_3$ (99%), and NaI (98%) were obtained from commercial suppliers and used as delivered. The ligands 2,6-$(MeOCH_2)_2C_6H_3Br$,[28] 1,3-$[^tBuOCH_2]_2C_6H_4$, and 2,6-$[^tBuOCH_2]_2C_6H_3Li$[15] were prepared according to literature procedures.

Synthesis of 2,6-$(MeOCH_2)_2C_6H_3SbCl_2$ (1). ^{n}BuLi (4.1 mL, 1.6 M hexane solution, 6.53 mmol) was added to a solution of 2,6-$(MeOCH_2)_2C_6H_3Br$ (1.6 g, 6.53 mmol) in 40 mL of THF at −80 °C. The resulting pale yellow solution was stirred for 2 h and then added dropwise to a solution of $SbCl_3$ (1.49 g, 6.53 mmol) in 100 mL of THF at −20 °C. The reaction mixture was allowed to reach room temperature, stirred for an additional 12 h, and evaporated in vacuo. The residue was extracted with 2 × 50 mL of CH_2Cl_2 and evaporated. Compound **1** was obtained after recrystalization from 1:5 $CHCl_3$/pentane as a white powder. Yield: 1.82 g (78%), mp 186−188 °C. Anal. Calcd for $C_{10}H_{13}Cl_2O_2Sb$ (MW 357.87): C, 33.56; H, 3.66. Found: C, 33.49; H, 3.64. Positive-ion ESI mass spectra: *m*/*z* 605 $[L^1SbOSbL^1OH]^+$; *m*/*z* 303 $[L^1SbOH]^+$, 100%; *m*/*z* 271 $[L^1SbOH - CH_3OH]^+$; *m*/*z* 241 $[L^1SbOH - HCOH - CH_3OH]^+$. Negative-ion ESI mass spectra: *m*/*z* 391 $[M + Cl]^-$, 100%. ^{1}H NMR (500 MHz, $CDCl_3$): 3.61 (6H, s, CH_3O), 4.88 (4H, s, OCH_2), 7.20 (2H, d, Ar-*H*3,5), 7.30 (1H, t, Ar-*H*4). ^{13}C NMR (125.76 MHz, $CDCl_3$): 58.60 (s, CH_3O), 75.33 (s, OCH_2), 125.30 (s, Ar-*C*3,5), 129.70 (s, Ar-*C*4), 145.86 (s, Ar-*C*2,6), 151.36 (s, Ar-*C*1).

Synthesis of 2,6-$(^tBuOCH_2)_2C_6H_3SbCl_2$ (2). A solution of 2,6-$(^tBuOCH_2)_2C_6H_3Li$ (1.45 g, 5.66 mmol) in 30 mL of THF was added dropwise to a solution of $SbCl_3$ (1.29 g, 5.66 mmol) in 100 mL of THF at −20 °C. The reaction mixture was allowed to reach room temperature, stirred for an additional 12 h, and evaporated in vacuo. The residue was extracted with 2 × 50 mL of toluene and evaporated. Compound **2** was obtained after recrystalization from 1:5 $CHCl_3$/pentane as a white powder. Yield: 1.88 g (75%), mp 119−120 °C. Anal. Calcd for $C_{16}H_{25}Cl_2O_2Sb$ (MW 442.03): C, 43.48; H, 5.70. Found: C, 43.49; H, 5.67. Positive-ion ESI mass spectra: *m*/*z* 793 $[L^2SbOSbL^2Cl]^+$; *m*/*z* 497 $[M + K + H_2O]^+$; *m*/*z* 481 $[M + Na + H_2O]^+$; *m*/*z* 405 $[M - Cl]^+$, 100%; *m*/*z* 349 $[M - Cl - \text{butene}]^+$; *m*/*z* 293 $[M - Cl - 2{*}\text{butene}]^+$; *m*/*z* 257 $[M - Cl - 2{*}\text{butene} - HCl]^+$. Negative-ion ESI mass spectra: *m*/*z* 475 $[M + Cl]^-$, 100%. ^{1}H NMR (500 MHz, $CDCl_3$): 1.57 (18H, s, br, $(CH_3)_3CO$), 5.03 (4H, s, br, OCH_2), 7.20 (2H, d, Ar-*H*3,5), 7.31 (1H, t, Ar-*H*4). ^{13}C NMR (125.76 MHz, $CDCl_3$): 28.21 (s, br, $(CH_3)_3CO$), 66.57 (s, br, OCH_2), 85.02 (s, br, *C*O), 123.06 (s, br Ar-*C*3,5), 129.09 (s, br, Ar-*C*4), 140.86 (s, br, Ar-*C*2,6), (Ar-*C*1) not found.

Synthesis of 2,6-$(MeOCH_2)_2C_6H_3SbI_2$ (3). NaI (0.42 g, 2.8 mmol) was added to a solution of 2,6-$(MeOCH_2)_2C_6H_3SbCl_2$ (0.5 g, 1.4 mmol) in 40 mL of acetone at room temperature. The resulting yellow suspension was stirred for 24 h, then the insoluble material was filtered off and the solvent was evaporated in vacuo. The residue was recrystallized from acetone to yield **3** as yellow crystals. Yield: 0.46 g (61%), mp 158−160 °C. Anal. Calcd for $C_{10}H_{13}I_2O_2Sb$ (MW 540.77): C, 22.21; H, 2.42; Found: C, 22.19; H, 2.39. Positive-ion ESI mass spectra: *m*/*z* 623 $[L^1SbOSbL^1OH + H_2O]^+$; *m*/*z* 605 $[L^1SbOSbL^1OH]^+$, 100%; *m*/*z* 413 $[M - I]^+$; *m*/*z* 321 $[L^1SbOH + H_2O]^+$; *m*/*z* 303 $[L^1SbOH]^+$; *m*/*z* 241 $[L^1SbOH - HCOH - CH_3OH]^+$. Negative-ion ESI mass spectra: *m*/*z* 667 $[M + I]^-$; *m*/*z* 127 $[I]^-$, 100%. ^{1}H NMR (500 MHz, $CDCl_3$): 3.78 (6H, s, CH_3O), 5.00 (4H, s, OCH_2), 7.22 (2H, d, Ar-*H*3,5), 7.37 (1H, t, Ar-*H*4). ^{13}C NMR (125.76 MHz, $CDCl_3$): 60.06 (s, CH_3O), 76.60 (s, OCH_2), 124.43 (s, Ar-*C*3,5), 130.03 (s, Ar-*C*4), 144.02 (s, Ar-*C*2,6), (Ar-*C*1) not found.

Synthesis of 2,6-$(^tBuOCH_2)_2C_6H_3SbI_2$ (4). Analogous procedure as for **3**: NaI (0.44 g, 2.94 mmol) and 2,6-$(^tBuOCH_2)_2C_6H_3SbCl_2$ (0.65 g, 1.47 mmol) give **4** as yellow powder. Yield: 0.58 g (63%), mp 119−120 °C. Anal. Calcd for $C_{16}H_{25}I_2O_2Sb$ (MW 624.94): C, 30.75; H, 4.03. Found: C, 30.72; H, 4.05. Positive-ion ESI mass spectra: *m*/*z* 497 $[M - I]^+$; *m*/*z* 441 $[M - I - \text{butene}]^+$; *m*/*z* 385 $[M-I - 2{*}\text{butene}]^+$, 100%; *m*/*z* 367 $[M - I - 2{*}\text{butene} - H_2O]^+$; *m*/*z* 257 $[M - I - 2{*}\text{butene} - HI]^+$. Negative-ion ESI mass spectra: *m*/*z* 751 $[M + I]^-$; 100%; *m*/*z* 127 $[I]^-$. ^{1}H NMR (500 MHz, $CDCl_3$): 1.71 (18H, s, $(CH_3)_3CO$), 5.10 (4H, s, OCH_2), 7.21 (2H, d, Ar-*H*3,5), 7.41 (1H, t, Ar-*H*4). ^{13}C NMR (125.76 MHz, $CDCl_3$): 28.34 (s, $(CH_3)_3CO$), 67.70 (s, OCH_2), 86.84 (s, *C*O), 123.25 (s, Ar-*C*3,5), 129.97 (s, Ar-*C*4), 141.52 (s, br, Ar-*C*2,6), 146.77 (s, Ar-*C*1).

Synthesis of 2,6-$(MeOCH_2)_2C_6H_3BiCl_2$ (5). ^{n}BuLi (2.8 mL, 1.6 M hexane solution, 4.49 mmol) was added to a solution of 2,6-$(MeOCH_2)_2C_6H_3Br$ (1.1 g, 4.49 mmol) in 40 mL of THF at −80 °C. The resulting orange solution was stirred for 2 h and then added dropwise to a solution of $BiCl_3$ (1.42 g, 4.49 mmol) in 100 mL of THF at −20 °C. The reaction mixture was allowed to reach room temperature, stirred for an additional 12 h, and evaporated in vacuo. The residue was washed with 20 mL of hexane, and the remaining solid was extracted with 2 × 50 mL of hot $CHCl_3$. Evaporation of the solvent gave **5** as white crystals. Yield: 1.38 g (69%), mp >250°C. Anal. Calcd for $C_{10}H_{13}Cl_2O_2Bi$ (MW 445.10): C, 26.99; H, 2.94. Found: C, 27.03; H, 2.96. Positive-ion ESI mass spectra: *m*/*z* 409 $[M - Cl]^+$, 100%; *m*/*z* 349 $[M - Cl - 2{*}HCOH]^+$.

---

[28] Markies, R. P.; Altink, R. M.; Villena, A.; Akkerman, O. S.; Bickelhaupt, F.; Smeets, W. J. J.; Spek, A. L. *J. Organomet. Chem.* **1991**, *402*, 289.

Negative-ion ESI mass spectra: *m/z* 479 [M + Cl]$^-$, 100%. ^{1}H NMR (500 MHz, $CDCl_3$): 3.74 (6H, s, CH_3O), 5.06 (4H, s, OCH_2), 7.43 (1H, t, Ar-*H*4), 7.75 (2H, d, Ar-*H*3,5). ^{13}C NMR (125.76 MHz, $CDCl_3$): 59.89 (s, CH_3O), 79.28 (s, OCH_2), 128.10 (s, Ar-*C*3,5), 129.17 (s, Ar-*C*4), 150.56 (s, Ar-*C*2,6), (Ar-*C*1) not found.

Synthesis of 2,6-(^{t}BuOCH$_2$)$_2$C$_6$H$_3$BiCl$_2$ (6). A solution of 2,6-[^{t}BuOCH$_2$]$_2$C$_6$H$_3$Li (1.64 g, 6.41 mmol) in 30 mL of THF was added dropwise to a solution of $BiCl_3$ (2.02 g, 6.41 mmol) in 100 mL of THF at −20 °C. The reaction mixture was allowed to reach room temperature, stirred for an additional 12 h, and evaporated in vacuo. The residue was extracted with 2 × 100 mL of toluene and evaporated. Compound **6** was obtained after recrystallization from 1:2 $CHCl_3$/pentane as a white powder. Yield: 2.47 g (73%), mp 155 °C. Anal. Calcd for $C_{16}H_{25}Cl_2O_2Bi$ (MW 529.26): C, 36.31; H, 4.76. Found: C, 36.35; H, 4.80. Positive-ion ESI mass spectra: *m/z* 493 [M − Cl]$^+$, 100%; *m/z* 437 [M − Cl − butene]$^+$; *m/z* 381 [M − Cl − 2*butene]$^+$. ^{1}H NMR (500 MHz, $CDCl_3$): 1.65 (18H, s, $(CH_3)_3CO$), 5.33 (4H, s, OCH_2), 7.47 (1H, t, Ar-*H*4), 7.82 (2H, d, Ar-*H*3,5). ^{13}C NMR (125.76 MHz, $CDCl_3$): 28.81 (s, $(CH_3)_3CO$), 72.00 (s, OCH_2), 84.12 (s, *C*O), 126.57 (s, Ar-*C*3,5), 129.00 (s, Ar-*C*4), 150.32 (s, Ar-*C*2,6), (Ar-*C*1) not found.

Synthesis of 2,6-(MeOCH$_2$)$_2$C$_6$H$_3$BiI$_2$ (7). NaI (0.42 g, 2.8 mmol) was added to a solution of 2,6-$(MeOCH_2)_2C_6H_3BiCl_2$ (0.62 g, 1.4 mmol) in 40 mL of acetone at room temperature. The resulting yellow suspension was stirred for 24 h, then the insoluble material was filtered off and the solvent was evaporated in vacuo. The residue was recrystallized from acetone to yield **7** as yellow crystals. Yield: 0.44 g (50%), mp >250 °C. Anal. Calcd for $C_{10}H_{13}I_2O_2Bi$ (MW 628.00): C, 19.13; H, 2.09. Found: C, 19.21; H, 2.12. Positive-ion ESI mass spectra: *m/z* 501 [M − I]$^+$; *m/z* 374 [M − 2*I]$^{+\cdot}$, 100%. Negative-ion ESI mass spectra: *m/z* 127 [I]$^-$. ^{1}H NMR (500 MHz, $CDCl_3$): 3.89 (6H, s, CH_3O), 5.17 (4H, s, OCH_2), 7.49 (1H, t, Ar-*H*4), 7.79 (2H, d, Ar-*H*3,5). ^{13}C NMR (125.76 MHz, $CDCl_3$): 61.42 (s, CH_3O), 81.71 (s, OCH_2), 127.45 (s, Ar-*C*3,5), 129.14 (s, Ar-*C*4), 149.56 (s, Ar-*C*2,6), (Ar-*C*1) not found.

Synthesis of 2,6-(^{t}BuOCH$_2$)$_2$C$_6$H$_3$BiI$_2$ (8). Analogous procedure as for **7**: NaI (0.42 g, 2.8 mmol) and 2,6-(^{t}BuOCH$_2$)$_2$C$_6$H$_3$BiCl$_2$

Table 2. Crystallographic Data for 1−8

	1	2	3	4
empirical formula	$C_{10}H_{13}Cl_2O_2Sb$	$C_{16}H_{25}Cl_2O_2Sb$	$C_{10}H_{13}I_2O_2Sb$	$C_{16}H_{25}I_2O_2Sb$
cryst syst	orthorhombic	monoclinic	orthorhombic	monoclinic
space group	*Pbca* (no. 61)	$P2_1/n$ (no. 14)	*Pbca* (no. 61)	$P2_1/c$ (no. 14)
a [Å]	13.3340(1)	10.6320(2)	14.0280(1)	8.4880(1)
b [Å]	8.5580(2)	12.3460(2)	8.0980(2)	23.6800(4)
c [Å]	22.0360(4)	14.8750(3)	25.4260(3)	9.9210(2)
α [deg]				
β [deg]		102.1500(11)		94.291(1)
γ [deg]				
Z	8	4	8	4
μ [mm^{-1}]	2.597	1.727	6.168	4.495
D_x [Mg m^{-3}]	1.891	1.538	2.487	2.087
cryst size [mm]	0.4 × 0.15 × 0.05	0.37 × 0.27 × 0.25	0.5 × 0.18 × 0.1	0.18 × 0.18 × 0.08
θ range [deg]	1−27.5	1−27.5	1−27.5	1−27.5
T_{min}, T_{max}	0.458,0.876	0.592, 0.635	0.257, 0.544	0.487, 0.746
no. of reflns measd	38 448	29 013	40 774	30 742
no. of unique reflns, R_{int}[a]	2885, 0.057	4374, 0.031	3312, 0.038	4556, 0.044
no. of obsd reflns [$I > 2\sigma(I)$]	2474	3950	3068	3989
no. of params	138	197	139	196
w_1/w_2[b]	0.0292/2.9583	0.0213/1.3235	0.0192/5.5192	0.0208/2.7328
S[c] all data	1.140	1.057	1.136	1.128
final *R*[d] indices [$I > 2\sigma(I)$]	0.026	0.023	0.021	0.025
wR2[d] indices (all data)	0.065	0.055	0.050	0.056
Δρ, max., min. [e Å^{-3}]	1.633, −1.041	0.596, −0.625	0.638, −0.756	0.747, −0.936

	5	6	7	8
empirical formula	$C_{20}H_{26}Cl_4O_4Bi_2$	$C_{16}H_{25}Cl_2O_2Bi$	$C_{10}H_{13}I_2O_2Bi$	$C_{16}H_{25}I_2O_2Bi$
cryst syst	triclinic	monoclinic	monoclinic	monoclinic
space group	$P\bar{1}$ (no. 2)	$P2_1/n$ (no. 14)	$C2/c$ (no. 15)	$P2_1/c$ (no. 14)
a [Å]	8.4310(3)	12.7470(2)	15.6080(5)	8.5780(2)
b [Å]	8.9130(2)	9.3590(2)	11.9450(3)	23.4510(3)
c [Å]	9.3080(3)	16.8500(3)	8.5850(3)	9.9950(2)
α [deg]	67.2420(17)			
β [deg]	78.6410(16)	109.464(1)	117.121(2)	94.550(1)
γ [deg]	77.3490(19)			
Z	1	4	4	4
μ [mm^{-1}]	14.523	9.586	16.692	11.879
D_x [Mg m^{-3}]	2.367	1.855	2.928	2.360
cryst size [mm]	0.25 × 0.2 × 0.1	0.25 × 0.18 × 0.15	0.25 × 0.15 × 0.1	0.22 × 0.12 × 0.075
θ range [deg]	1−27.5	1−27.5	1−27.5	1−27.5
T_{min}, T_{max}	0.098, 0.342	0.161, 0.329	0.048, 0.227	0.226, 0.365
no. of reflns measd	10 467	25 605	9598	30 754
no. of unique reflns, R_{int}	2853, 0.052	4344, 0.092	1637, 0.085	4582, 0.053
no. of obsd reflns [$I > 2\sigma(I)$]	2752	3855	1589	3888
no. of params	139	197	72	197
w_1/w_2[b]	0.0264/0.9244	0.087/3.5904	0.0305/5.7101	0.0301/5.5227
S[c] all data	1.096	1.066	1.122	1.070
final *R*[d] indices [$I > 2\sigma(I)$]	0.022	0.0275	0.026	0.030
wR2[d] indices (all data)	0.055	0.069	0.068	0.069
Δρ, max., min. [e Å^{-3}]	1.312, −2.484	2.185, −1.779	1.340, −1.237	1.670, −1.608

[a] $R_{int} = \sum|F_o^2 - F_{o,mean}^2|/\sum F_o^2$. [b] Weighting scheme: $w = [\sigma^2(F_o^2) + (w_1P)^2 + w_2P]^{-1}$, where $P = [\max(F_o^2) + 2F_c^2]$. [c] $S = [\sum(w(F_o^2 - F_c^2)^2)/(N_{diffrs} - N_{params})]^{1/2}$. [d] $R(F) = \sum||F_o| - |F_c||/\sum|F_o|$, $wR(F^2) = [\sum(w(F_o^2 - F_c^2)^2)/(\sum w(F_o^2)^2)]^{1/2}$.

(0.74 g, 1.4 mmol) give **8** as a yellow powder. Yield: 0.57 g (57%), mp 158−160 °C. Anal. Calcd for $C_{16}H_{25}I_2O_2Bi$ (MW 712.17): C, 26.99; H, 3.54. Found: C, 27.04; H, 3.57. Positive-ion ESI mass spectra: m/z 713 $[M + H]^+$; m/z 585 $[M - I]^+$, 100%; m/z 529 $[M{-}I - \text{butene}]^+$; m/z 529 $[M - I - \text{butene}]^+$; m/z 473 $[M - I - 2{*}\text{butene}]^+$; m/z 401 $[M + H - 2{*}I\text{-butane}]^+$; m/z 345 $[M + H - 2{*}I - \text{butene} - \text{butane}]^+$. Negative-ion ESI mass spectra: m/z 839 $[M + I]^-$, 100%; m/z 127 $[I]^-$. ^{1}H NMR (500 MHz, $CDCl_3$): 1.63 (18H, s, $(CH_3)_3CO$), 5.28 (4H, s, OCH_2), 7.51 (1H, t, Ar-*H*4), 7.80 (2H, d, Ar-*H*3,5). ^{13}C NMR (125.76 MHz, $CDCl_3$): 28.69 (s, $(CH_3)_3CO$), 72.52 (s, OCH_2), 84.67 (s, *C*O), 126.81 (s, Ar-*C*3,5), 128.96 (s, Ar-*C*4), 150.25 (s, Ar-*C*2,6), (Ar-*C*1) not found.

X-ray Crystallographic Study. The details of the crystal structure determination and refinement for compounds **1**−**8** are given in Table 2. Suitable single crystals of **1**−**8** were mounted on a glass fiber with silicon oil and measured on a KappaCCD four-circle diffractometer with CCD area detector by monochromatized Mo Kα radiation ($\lambda = 0.71073$ Å) at 150(2) K. The numerical absorption corrections[29] from the crystal shape were applied for all crystals. The structures were solved by the direct method (SIR97[30]) and refined by a full matrix least squares procedure based on F^2 (SHELXL97[31]). Hydrogen atoms were fixed into idealized positions (riding model) and assigned temperature factors $H_{iso}(H) = 1.2U_{eq}$(pivot atom); for the methyl moiety a multiple of 1.5 was chosen. The final difference maps displayed no peaks of chemical significance, as the highest peaks and holes are in close vicinity to heavy atoms.

Crystallographic data for structural analysis have been deposited with the Cambridge Crystallographic Data Centre, CCDC nos. 609167−609174 for **1**−**8**, respectively. Copies of this information may be obtained free of charge from The Director, CCDC, 12 Union Road, Cambridge CB2 1EY, UK (fax: +44-1223-336033; e-mail: deposit@ccdc.cam.ac.uk; or www: http://www.ccdc.cam.ac.uk).

Acknowledgment. The authors thank the Ministry of Education of the Czech Republic (projects VZ 0021627501 and LC523) for financial support. R.J. acknowledges the support of grant project No. MSM0021627502 sponsored by the Ministry of Education, Youth and Sports of the Czech Republic.

Supporting Information Available: The ln *K* vs T^{-1} plot for *cis*−*tran*s equilibrium in $CDCl_3$ solution of **2**. Tables of all crystal data and structure refinement, atomic coordinates, anisotropic displacement parameters, and geometric data for compounds **1**−**8**. This material is available free of charge via the Internet at http://pubs.acs.org.

OM060489Q

---

(29) Coppens, P.; Ahmed, F. R.; Hall, S. R.; Huber, C. P. *Crystallographic Computing*; Munksgaard: Copenhagen, 1970; p 255.

(30) Altomare, A.; Cascarano, G.; Giacovazzo, C.; Guagliardi, A.; Burla, M. C.; Polidori, G.; Camalli, M. *J. Appl. Crystallogr.* **1994**, *27*, 435.

(31) Sheldrick, G. M. *SHELXL97*; University of Göttingen: Germany, 1997.